IEEE Access
Multidisciplinary ⋮ Rapid Review ⋮ Open Access Journal

Received March 10, 2020, accepted March 17, 2020, date of publication March 23, 2020, date of current version May 1, 2020.

Digital Object Identifier 10.1109/ACCESS.2020.2982776

Maximizing Transfer Distance for WPT via Coupled Magnetic Resonances by Coupling Coils Design and Optimization

YANG LI, SHAN JIANG, JIA-MING LIU, XIN NI, RUI WANG, AND JING-NAN MA
Tianjin Key Laboratory of Advanced Electrical Engineering and Energy Technology, Tiangong University, Tianjin 300387, China

Corresponding author: Shan Jiang (13821058157@163.com)

This work was supported in part by the National Key R&D Program of China under Grant 2017YFB1201003-022, in part by the National Natural Science Foundation of China under Grant 51577133, Grant 51877151, Grant 51607121, and Grant 51807138, in part by the Natural Science Foundation of Tianjin under Grant 18JCQNJC70500, and in part by the Program for Innovative Research Team in University of Tianjin under Grant TD13-5040.

ABSTRACT The technology of wireless power transfer via coupled magnetic resonances (CMR-WPT) has a good transfer performance in the ''middle range'', but it is far from satisfying the application requirements in practice. To achieve a longer transfer distance, coils are usually complicatedly designed, making the system unwieldy and costly. Based on the intuitive and easily adjustable coil parameters, a design and optimization method was proposed in this paper, which can realize the minimum size coil that meets the requirements at 6.78 MHz. First, an equivalent model of the CMR-WPT system was developed, and the influences of coil parameters on the effective transfer distance and power transfer efficiency (PTE) were analyzed, indicating that the effective transfer distance and PTE were not always proportional to the coil radius, the number of turns or the pitch. Then, the coil impedance and the quality factor of different coils were calculated. In addition, the influence degree of coil parameters on the transfer performance was also compared using variable control. Finally, an experimental platform was built, and experimental results agreed well with the simulation results.

INDEX TERMS Coupled magnetic resonances, design and optimization, coil parameters, effective transfer distance, power transfer efficiency.

I. INTRODUCTION

The technology of wireless power transfer via coupled magnetic resonances (CMR-WPT) was put forward at MIT [1], with many advantages such as a long transfer distance, a high power transfer efficiency (PTE), and low requirement for directivity [2]–[4]. In addition, it can avoid many hidden risks in power supply compared with the traditional technology [5]–[7]. As a result, it has been applied in various fields, including portable devices [8], medical implants [9], and electric vehicles [10].

The point at which the load received power decreases significantly with the increase in transfer distance is defined as the critical point, and the distance between the Tx coil and the critical point is called effective transfer distance, which is also termed as the efficient range for the CMR-WPT system [11], [12]. By increasing the effective transfer distance, one can greatly promote the commercialization of CMR-WPT technology. Up to now, several related methods have been introduced as follows.

1) Adding an auxiliary circuit or extra coils for realizing a long transfer distance. A parity-time symmetric circuit was designed to ensure that a high transfer efficiency was consistent within 1 m [13]. In [14] and [15], the proposed system consisted of a series of sub-coils for realizing a high PTE at different transfer distances. The parallel-wire coils were used and the ratio between currents on the two wires were controlled to achieve a longer transfer distance [16]. Note that these methods are complicated and the corresponding costs are higher.
2) Adopting new multi-coil structures. The intermediate-resonator provided a simple approach to improve the transfer distance [17]–[19]. In [20], an inner coil was incorporated in the Tx coil to achieve a higher efficiency at a long transfer distance. In [21], two strongly coupled resonators were embedded within a Tx (Rx)

The associate editor coordinating the review of this manuscript and approving it for publication was Giambattista Gruosso.

This work is licensed under a Creative Commons Attribution 4.0 License. For more information, see https://creativecommons.org/licenses/by/4.0/

APPLE 2025
Masimo v. Apple
IPR2023-00734

device to maximize the coupling coefficient. However, the multi-coil structures are inconvenient and take up a larger space.

3) Designing and optimizing the coupling coil. In [22], a design and optimization method for the small coil used in implantable medical devices was proposed. An optimizable coil configuration and a circuit model were proposed to increase the transfer distance [23]. A method with the smallest quality factor for coil was put forward, thus realizing the requirement for efficiency and a long transfer distance [24]. The above methods are applicable, but they are not capable of increasing the transfer distance significantly. In the coil design, the coil parameters (e.dg., coil radius r, the number of turns N, and pitch a) are the most intuitive and easiest to adjust, but the related research is unsystematic. Moreover, the variation ranges of coil parameters and transfer distance are limited, which is weak in fully guiding the CMR-WPT system design.

In this paper, an equivalent model of CMR-WPT system was constructed at first. Second, simulation software was used to study the influences of coil parameters on the effective transfer distance and PTE. Third, two design and optimization flowcharts for increasing the transfer distance and PTE at 6.78 MHz were proposed. Finally, an experimental platform was built to verify the simulation results. Moreover, the application of CMR-WPT technology which in the fields of smart home, smart robot and high-speed rail can be promoted by using the research results of this paper to design the coupling coil reasonably.

II. GUIDELINES FOR MANUSCRIPT PREPARATION

The schematic and equivalent circuit of a CMR-WPT system powered by an RF power generator at 6.78 MHz are shown in Fig. 1.

Based on the Kirchhoff's voltage law (KVL), the following equations can be obtained, i.de.,

$$\begin{cases} U_s = (R_1 + j\omega L_1 + \dfrac{1}{j\omega C_1})I_1 - j\omega M I_2 \\ 0 = (R_2 + R_L + j\omega L_2 + \dfrac{1}{j\omega C_2})I_2 - j\omega M I_1 \end{cases} \tag{1}$$

Through calculations, the received power of load and system efficiency can be expressed as

$$P_L = \frac{U_S^2 R_L (\omega M)^2}{\left[(R_0 + R_1)(R_2 + R_L) + (\omega M)^2\right]^2} \tag{2}$$

$$\eta = \frac{R_L (\omega M)^2}{\left[(R_0 + R_1)(R_2 + R_L) + (\omega M)^2\right](R_2 + R_L)} \tag{3}$$

When the WPT system is completed, the parameters (e.dg., the exciting voltage, frequency, internal resistance, load, and coil impedance) are fixed. Therefore, the received power can be regarded as a function of M, and

$$M^* = \frac{\sqrt{(R_0 + R_1)(R_2 + R_L)}}{\omega} \tag{4}$$

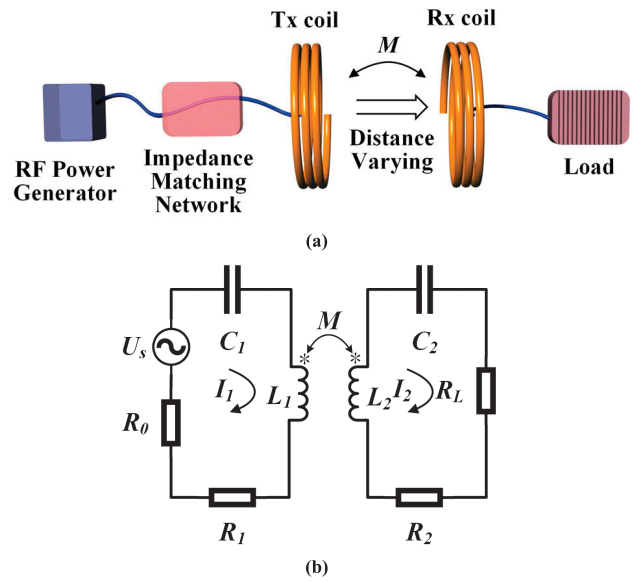

FIGURE 1. Schematic and equivalent circuit of WPT system. (a) Schematic. (b) Equivalent circuit.

The received power reaches its maximum (i.de., M^* in (4)), so the critical point of CMR-WPT system is reached and the transfer distance corresponding to M^* is the effective transfer distance. The next step is to calculate the value of M^*. A multiloop circular coil (e.dg., a spiral coil) is equivalently replaced by a concentric circular multiloop coil, and the mutual inductance between single circular coils are calculated as [25]:

$$M_{ij} = \mu_0 \sqrt{r_i r_j} \frac{2}{\alpha} \left[\left(1 - \frac{\alpha^2}{2}\right) K(\alpha) - E(\alpha) \right] \tag{5}$$

With

$$\alpha = 2\sqrt{\frac{r_i r_j}{(r_i + r_j)^2 + d^2}} \tag{6}$$

$$M = \sum_{i=1}^{N_1} \sum_{j=1}^{N2} M_{ij} \tag{7}$$

where μ_0 is permeability of vacuum; r_i and r_j are coil radiuses; d is transfer distance; and $K(\alpha)$ and $E(\alpha)$ are elliptic integrals of modulus α. By combining formulas (4)–(7), the value of effective transfer distance can be obtained, at which the PTE will be analyzed further. The maximum achievable PTE ($\eta_{\max}$) is given as [26]:

$$\eta_{\max} = \frac{\varphi^2}{(1 + \sqrt{1 + \varphi^2})^2} \tag{8}$$

where

$$\varphi = \sqrt{\frac{(\omega M^*)^2}{R_1 R_2}}$$

According to formulas (4)–(8), the coil radius and impedance can be considered as factors that mainly affect the effective transfer distance as well as PTE. It should be pointed out that

TABLE 1. P parameters of coils with different shapes.

	Plane spiral	Plane square	Barrel spiral
r(cm)	15	15	15
N	8	7	7
a(mm)	5.12	5.12	5.12
Inductance(μH)	28.412	28.359	28.160
Resistance(mΩ)	35.407	35.540	35.011

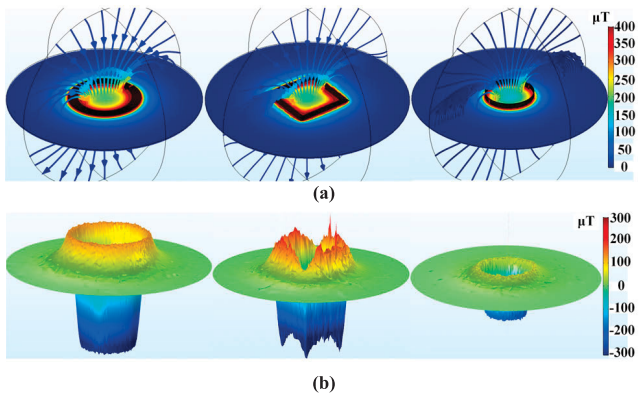

FIGURE 2. Simulation results of coils of different shapes (a) Distribution of magnetic field. (b) Distribution of height.

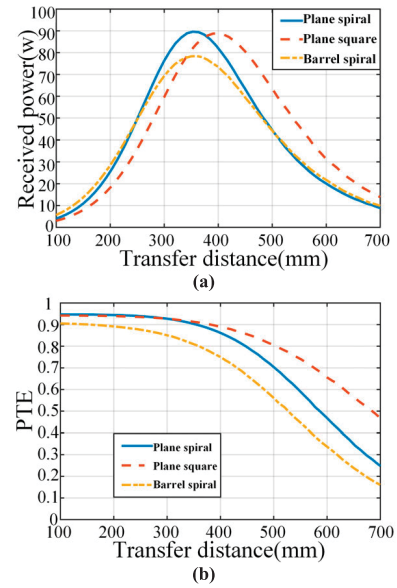

FIGURE 3. Distance characteristics of coils of different shapes. (a) Rx power. (b) PTE.

the calculations of d and $\eta_{\max}$ are usually complicated, and other factors (e.dg., the shape, number of turns N, and pitch a) cannot be expressed.

III. DESIGN AND OPTIMIZATION FOR COUPLING COILS

The resonance circuit and the propagation of electromagnetic waves around coupling coils can be calculated by the RF module in COMSOL, so the RF module is chosen. The frequency and load are set to 6.78 MHz and 50 Ω, respectively, and the Tx and Rx coils are tuned by two series capacitances.

A. SIMULATION OF COIL SHAPE

The plane spiral, plane square and barrel spiral are set up with the same coil parameters and similar inductances, as listed in Table 1. At 6.78 MHz, the magnetic field distribution and height of the magnetic field component along the z-axis are shown in Fig. 2, the sections and streamlines (magnetic field lines) indicate the magnetic field distribution in the transverse and longitudinal directions of coils, respectively.

From Fig. 2(a), it can be seen that in the case of the same inductance, the magnetic field of plane spiral is the strongest while the distribution in the vertical direction is relatively uniform and wide. By contrast, the magnetic field around plane square is weak, and it is widely distributed in the horizontal direction. The magnetic field of barrel spiral is dispersed in the vertical and horizontal directions. As can be seen from Fig. 2(b), there are large differences among three coils. The magnetic field of plane and barrel spirals on the z-axis are continuous and smooth, with no fluctuations. However, the magnetic field of plane square has a corner effect, resulting in uneven distribution and more serious fluctuations. Because the magnetic field (along the z-axis) generated by two adjacent current-carrying wires do not overlap in the four corners, the magnetic strengths at the four corners are much weaker than that in the middle of the coil.

Parameterized scanning is performed at the transfer distance for analyzing the influences of coil shape on the distance characteristics, as shown in Fig. 3.

As can be seen from Fig. 3, the effective transfer distance of plane spiral, plane square and barrel spiral are 36, 39 and 35 cm, at which the PTEs are 90.11%, 89.55% and 80.00%, respectively. The effective transfer distances of the three systems have less variations, but there is a 10% gap in PTE. To further explain this phenomenon, mutual inductance and normalized power are calculated, as shown in Fig. 4.

From Fig. 4(a), it can be seen that when the transfer distance is less than 30 cm, the mutual inductances of the plane square, plane spiral, and barrel spiral are in an decreasing order. When transfer distance is longer than 30 cm, the mutual inductances of three coils are not much different and keep small values. Compared with the inductively coupled power transfer, CMR-WPT is of loose coupling, and its coupling coefficient and mutual inductance are small.

Moreover, the normalized power in the range of 6.08–7.48 MHz is calculated, as shown in Fig. 4(b). Based on the passband principle, the sharpness of curve is directly proportional to the quality factor. In the case of the same inductance, the quality factors of planar square, planar spiral and barrel spiral are in an decreasing order. According to $Q = \omega L/RQ = \omega L/R$, when the frequency and inductance are constant, the coil impedance will play a decisive role in the quality factor. The planar square has a higher quality factor, so its effective transfer distance is longer. From Figs. 2 and 3, it can be seen that the plane spiral and plane square have better transfer performances.

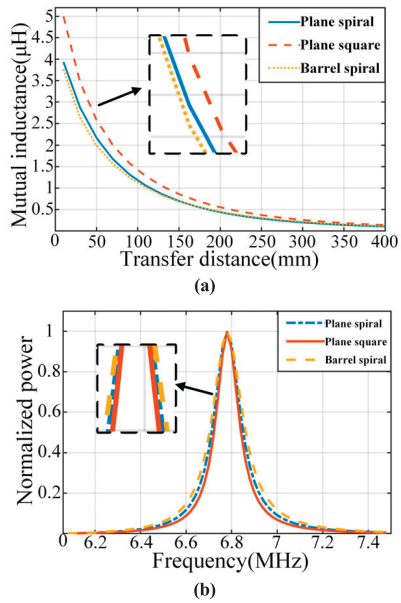

FIGURE 4. Mutual inductance M and quality factors of coils of different shapes. (a) M. (b) quality factor.

TABLE 2. Coil parameters in simulations.

Parameter	Value
N	10
a (mm)	2.5
Wire diameter (mm)	2.12
r (cm)	5/10/15/20/25
Resistance(mΩ)	19.56/38.90/59.53/89.86/127.93

B. SIMULATION OF COIL RADIUS

By changing the inner diameters of Tx and Rx coils, one can study the influences of coil radius on the effective transfer distance and PTE. The simulated coil parameters are listed in Table 2, and the simulated results are shown in Fig. 5.

In Fig. 5(a), the effective transfer distances of the system with different radiuses are 7, 29, 44, 60 and 38 cm, respectively, and the effective transfer distance increases at first but then decreases. In Fig. 5(b), the PTEs of five systems at effective transfer distance are 96.54%, 85.86%, 82.87%, 73.23% and 89.74%, respectively, and the PTE decreases obviously when the transfer distance exceeds its effective value. The mutual inductance in different systems are calculated, as shown in Fig. 6.

Fig. 6 shows that there are large differences in mutual inductance when the transfer distance is less than 30 cm. If the distance is longer than 30 cm, the difference will become small. Therefore, it should be pointed out that the effect of mutual inductance is reduced at a longer transfer distance, and there are other factors affecting the transfer performance of the CMR-WPT system. To explain the reason why the effective transfer distance is reduced, the radiuses are set to 10, 20, 30 cm, and the magnetic field intensity and the section with magnetic induction lines are calculated, as shown in Fig.7.

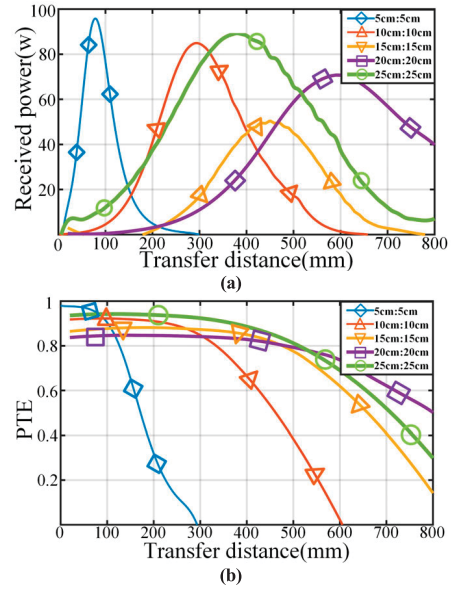

FIGURE 5. Distance characteristics of system with different radiuses. (a) Received power. (b) PTE.

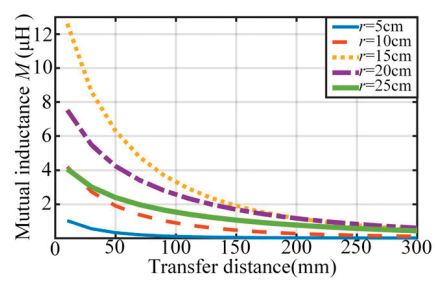

FIGURE 6. Mutual inductance with different radiuses.

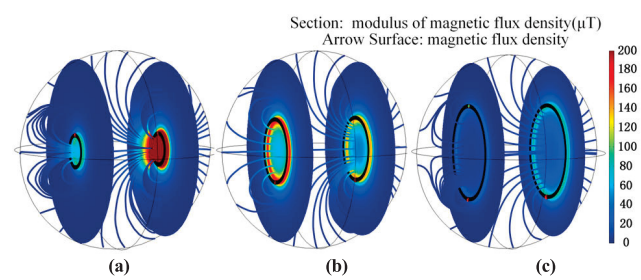

FIGURE 7. Magnetic field of system with different radiuses. (a) $r = 10$ cm. (b) $r = 20$ cm. (c) $r = 30$ cm.

The system frequency, excitation voltage, and load are set as the same values, with a transfer distance of 55 cm.

In Fig. 7, the Tx coil is on the right while the Rx coil is on the left. From the vertical section, it can be seen that the magnetic field intensity of Rx coil in Fig. 7(b) is significantly stronger than that in 7(a) and (c). Therefore, the system with radius of 20 cm is more efficient. In addition, more magnetic induction lines pass through the Rx coil in Fig. 7(b) than in 7(a) and (c). If the coil radius is too small, lots of magnetic induction lines will form a loop near the Tx coil, thereby

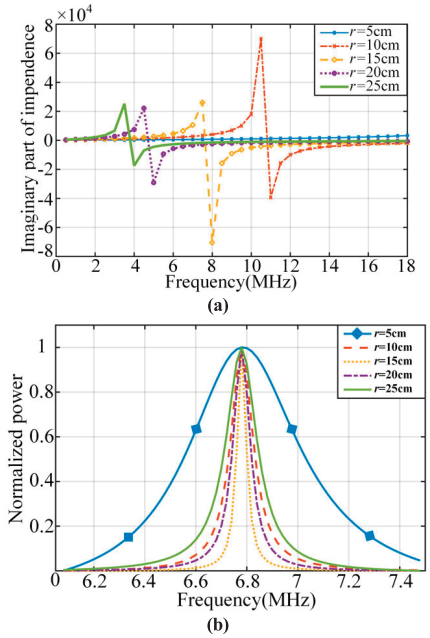

FIGURE 8. Frequency characteristics of different coils. (a) Imaginary part of impendence without tuning. (b) Normalized power.

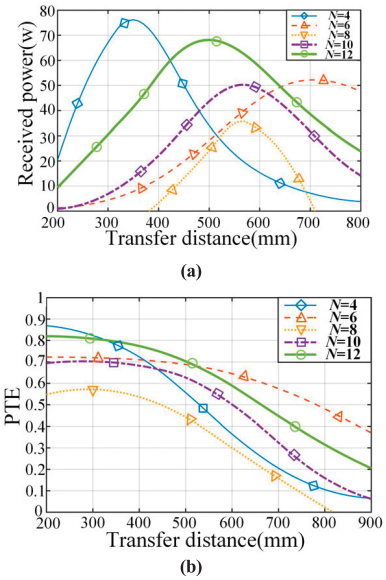

FIGURE 9. Distance characteristics with pitch of 2.5 mm. (a) Received power. (b) PTE.

TABLE 3. Effective transfer distances and PTE in figs.11–13.

	a=6.5	*a*=10.5	*a*=14.5
N=4	25cm/97.68%	23cm/97.32%	22cm/97.38%
N=6	44cm/79.78%	33cm/95.74%	31cm/96.00%
N=8	47cm/74.13%	45cm/90.13%	36cm/94.88%
N=10	57cm/42.68%	50cm/89.51%	39cm/93.84%
N=12	55cm/60.07%	54cm/86.90%	40cm/93.22%

increasing the magnetic flux leakage. The magnetic induction line will become sparse and the magnetic field will thus be reduced if the radius is too large. As a result, it can be inferred that a too small of too large coil will deteriorate the performance of the CMR-WPT system.

The frequency characteristics of coils after tuning are shown in Fig. 8.

When a sudden change from positive to negative occurs in the imaginary part of the coil impedance, the frequency at the abrupt point is approximatively the resonant frequency of the coil. In Fig. 8(a), the self-resonant frequency of the coil with radiuses of 15 and 20 cm are close to 6.78 MHz, while those with other radiuses are far away. After tuning, the resonant frequency of coils is 6.78 MHz, and the quality factors of different coils are calculated, as shown in Fig. 8(b). The quality factors of the two coils with radiuses of 15 and 20 cm are higher, and these two systems achieve a longer effective transfer distance, as shown in Fig. 5(a). However, a too small or too high quality factor (e.dg., in the case with radius of 15 cm) will bring many problems, such as the difficulty in tuning, higher requirements for electronic devices, and received power and PTE that are sensitive to the changes in resonant frequency and transfer distance. Moreover, if the imaginary part cannot be completely eliminated through tuning, the reactive current will generate active loss in the coil and further reduce the efficiency. Therefore, it is necessary to design the coil radius reasonably.

C. SIMULATION OF THE NUMBER OF TURNS AND THE PITCH

After the radius is determined, the number of turns and the pitch should be studied further. In this section, the pitch is 2.5 mm, the coil radius is 20 cm, and the number of turns is 4–12 with a step size of 2. The simulation results are shown in Fig. 9.

From Fig. 9(a), it can be seen that when the numbers of turns are 4, 6, 8, 10, 12, the effective transfer distances are 35, 71, 57, 56 and 50 cm, respectively. With the growing number of turns, the effective transfer distance increases at first but then decreases gradually. In Fig. 9(b), the PTEs of five systems at the effective transfer distance are 78.38%, 56.55%, 34.85%, 55.6% and 70.23%, respectively. When the pitch is 2.5 mm, the PTE changes distinctly with the increase in transfer distance. And the decline of PTE will be more serious if the transfer distance is longer than the effective transfer distance.

Multiple simulations are also conducted, as shown in Figs. 10–12.

Form the above analyses, it can be seen that when the effective transfer distance expands with the increase in the number of turns, PTE tends to decrease. The smaller the pitch, the more obviously the PTE will decrease. Moreover, if the effective transfer distance expands to its maximum while the number of turns increase continuously, PTE will increase. When the pitches are 10.5 and 14.5 mm respectively, the effective transfer distance is proportional to the number of turns, and the drop point does not exist. Besides, the PTE can

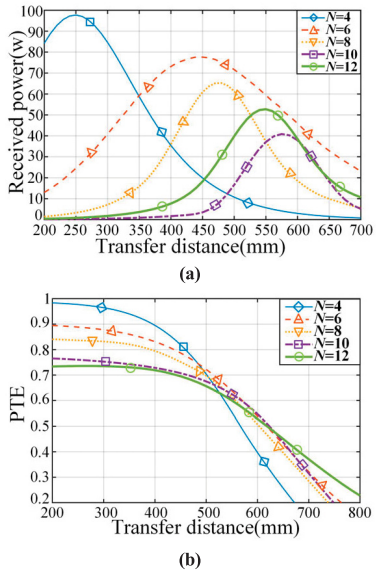

FIGURE 10. Distance characteristics with pitch of 6.5 mm. (a) Received power. (b) PTE.

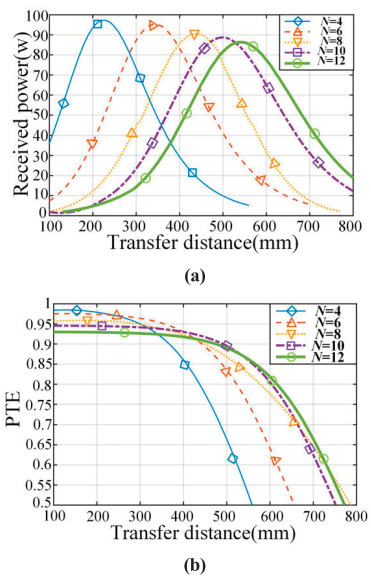

FIGURE 11. Distance characteristics with pitch of 10.5 mm. (a) Received power. (b) PTE.

be maintained at a high value before reaching the effective transfer distance, and the variation degree of PTE is minor when the number of turns changes, but the values of effective transfer distance are similar.

The values of the above changes are due to the coil impedance, and the changes in the number of turns and pitch deeply affect the coil impedance and quality factor [21], [23]. To give a more accurate conclusion, the coil impedance is calculated at 6.78 MHz without tuning, and the results are shown below.

Except for Fig. 13(a), the trends of real part in Fig. 13 firstly increase but then decrease. In Fig. 14(b), (c), and (d), there

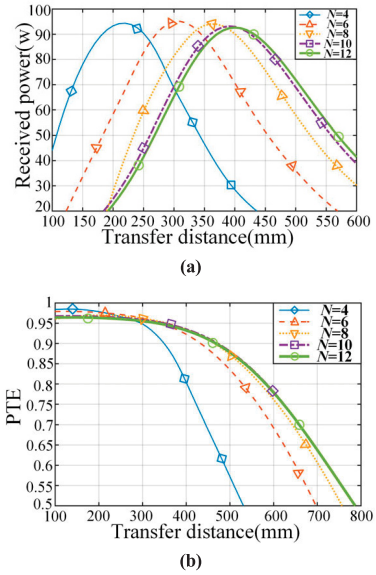

FIGURE 12. Distance characteristics with pitch of 14.5 mm. (a) Received power. (b) PTE.

is a sudden change in the imaginary part of coil impedance with the increase in pitch. In the megahertz range, the coil is under parallel resonance, and the two-port network (coupling coil) viewed from the power supply is equivalent to an open circuit. As a result, the real part of the coil impedance has a particularly large value in the process of changing the number of turns and the pitch, as shown in Fig. 13, where the curves of imaginary part present a mutation between positive and negative, as shown in Fig. 14. At this point, the self-resonant frequency of the coil is very close to 6.78 MHz and its quality factor is higher. Considering Figs. 10–12, when the self-resonant frequency of the coil is close to 6.78 MHz, the effective transfer distance of the WPT system will be longer. The above analyses also verify the influences of coil radius on the effective transfer distance, as shown in Fig. 9.

The comprehensive analysis shows that, at 6.78 MHz, the number of turns will not be directly proportional to the effective transfer distance when the pitch is small. Besides, the PTE is not improved. A larger number of turns leads to a higher inductance of coils, a deteriorated radiation magnetic field around coil, uncontrollable leakage inductance of coil, and a growing loss of AC resistance. According to the specific requirements for effective transfer distance and PTE in practical engineering, the number of turns and the pitch should be adjusted reasonably.

D. COMPARISON OF INFLUENCES OF COIL PARAMETERS, AND FLOWCHARTS OF DESIGN AND OPTIMIZATION

Form the above analyses, it can be seen that different coil parameters can seriously affect the effective transfer distance and the PTE of the CMR-WPT system. To further guide the design of coils, the influences of coil parameters on the transfer performance are compared. With the intermediate in a series of data taken as a reference (0,0), the corresponding

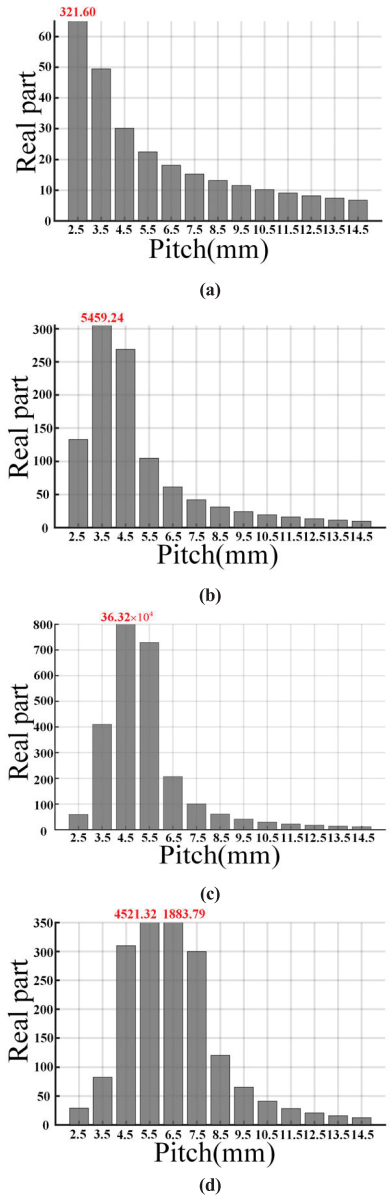

FIGURE 13. Real part of different coils. (a) $N = 6$. (b) $N = 8$. (c) $N = 10$. (d) $N = 12$.

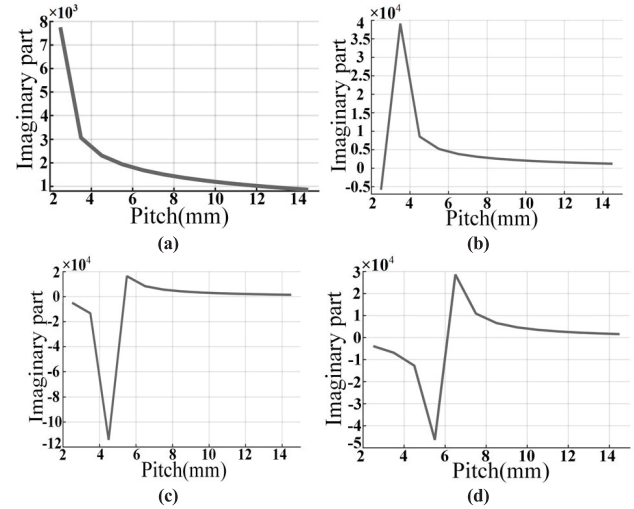

FIGURE 14. Imaginary part of different coils. (a) $N = 6$ (b) $N = 8$. (c) $N = 10$. (d) $N = 12$.

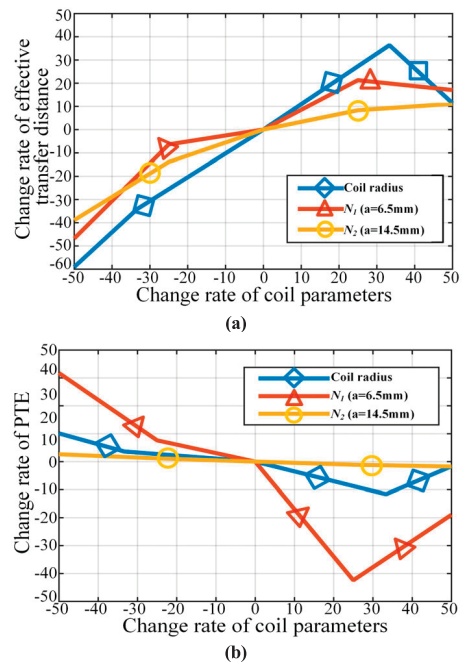

FIGURE 15. Comparison of influences due to different coil parameters. (a) Influences on effective transfer distance. (b) Influences on PTE.

results are shown in Fig. 15. Here, the pitch is represented by a, and the PTE in Fig. 15(b) is a value under effective transfer distance.

On the one hand, the coil shape affects the distribution of magnetic field mostly. On the other hand, the actual product requirements and the space available should be considered. Therefore, only the change rate of coil radius, the number of turns and the pitch are calculated.

In Fig. 15(a), there is a larger slope with the curve of coil radius, meaning that the coil radius affects the effective transfer distance more seriously than the number of turns ($a = 6.5$ mm/14.5 mm). The increase in the pitch ($a = 6.5 - 4.5$ mm) reduces the slope of the curve for the number of turns, i.de., changing the pitch can reduce the effect of the changes in the number of turns. Moreover, the inflection of curve indicates that the effective transfer distance is shortened.

In Fig. 15(b), the trends of three curves are opposite to those in Fig. 15(a), meaning that the PTE will be reduced when the effective transfer distance increases. When the pitch is small ($a = 6.5$ mm), the increase in the number of turns has the largest impact on PTE, but increasing the pitch ($a = 14.5$ mm) will reduce that impact. In addition, the inflection of the curve shows that the PTE increases.

It can be concluded that the coil radius (r) has the largest influence on the transfer performance of the CMR-WPT

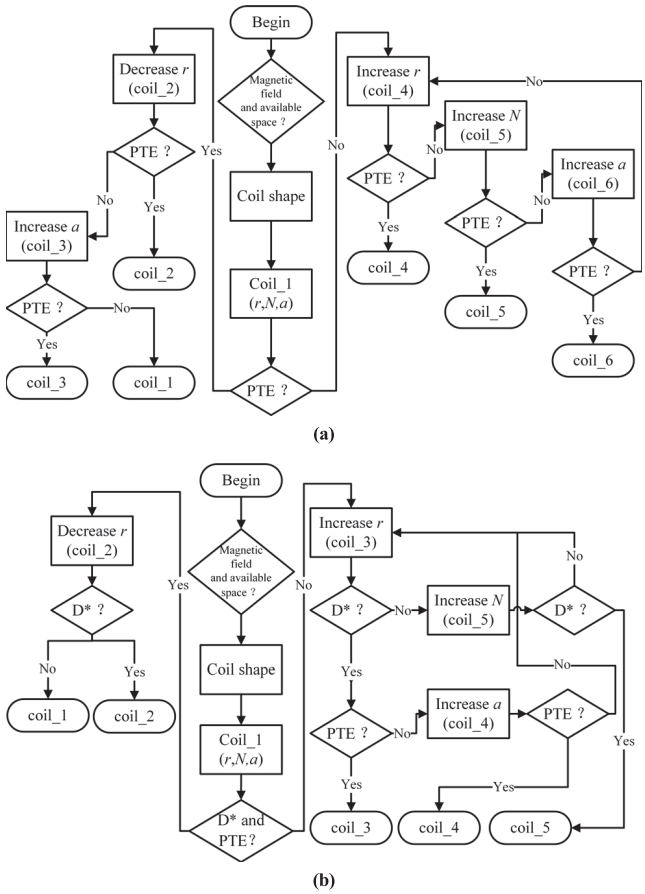

FIGURE 16. Flowcharts of design and optimization. (a) At invariable transfer distance. (b) At variable transfer distance.

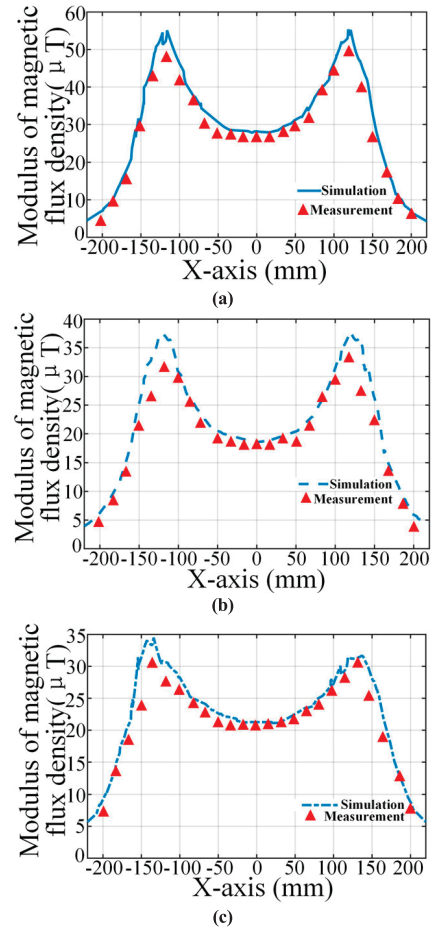

FIGURE 17. Modulus of magnetic flux density. (a) Plane spiral. (b) Plane square. (c) Barrel spiral.

system, followed by the number of turns (N) and the pitch, (a) sequentially. From the above analyses, the design and optimization processes of coils at 6.78 MHz, which meet the actual engineering design requirements for the smallest possible size, are summarized in Fig.16.

The difference between Fig. 16(a) and (b) is that the transfer distance in Fig. 16(a) is determined while the longest distance which meets the requirement for PTE is realized in Fig. 16(b). In addition, all the above CMR-WPT systems shown in Fig. 16 are always resonant at 6.78 MHz.

IV. IMPLEMENTATION OF CMR-WPT SYSTEM AND EXPERIMENTAL RESULTS

The plane spiral, plane square and barrel spiral coils were manufactured for verifying the simulation results of magnetic field distribution. The modulus of magnetic field density was measured using a 3D visualization electromagnetic field measuring device.

In the process of setting up the experimental platform, the center frequency of a spectrum analyzer (AARONIA, NF-5035S) was 6.78 MHz, and the signal generator was connected to the NF power amplifier (with internal resistance of 50 Ω) to provide a high-frequency power. The experimental results were shown in Fig. 17.

TABLE 4. Parameters of coils with different radiuses.

Radius/cm	Inductance/μH	Resistance/mΩ
5	9.90	20.43
10	23.50	34.50
15	39.23	60.21
20	57.80	113.62
25	79.54	159.84

As can be seen from Fig. 17, the magnetic field strength of planar spiral coil in the horizontal direction was the maximum, followed by planar square and barrel spiral, sequentially. However, for the barrel spiral, the difference at the extreme point of magnetic field strength was small. Moreover, there were slight differences between the experimental and simulated data. Ignoring these errors, the simulation curves were in good agreement with the experimental results.

An experimental platform based on simulations was built to verify the influences of coil parameters on the effective transfer distance of the CMR-WPT system.

In Fig. 18, the different coil radiuses were selected, and the coil parameters extracted from measurement data by a vector network analyzer are listed in Table 4.

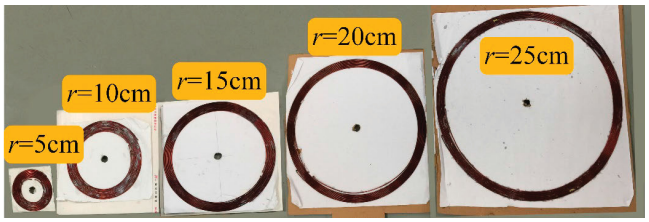

FIGURE 18. The coils with different radiuses.

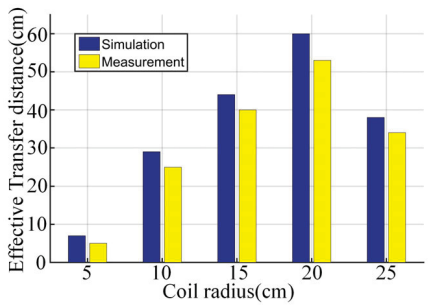

FIGURE 19. Experimental results of effective transfer distance.

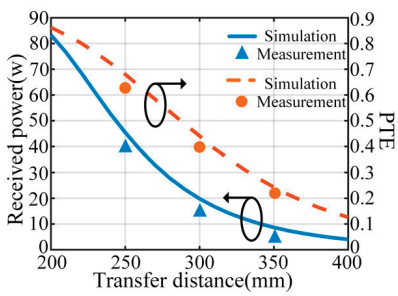

FIGURE 20. Simulation and experimental results.

TABLE 5. Parameters of coils in [19] and this paper.

	r Tx/Rx(cm)	N Tx/Rx	a Tx/Rx(mm)	PTE at 30 cm
[19]	10/5	9/7	4/0.5	39%
This paper	10/6	15/13	4.5/2.5	40.21%

Based on repeated experiments, the measurement results are shown in Fig. 19.

Fig. 19 shows that the experimental data have the same trend as the simulation results. However, there are differences, which may be due to the contact resistance at the solder joint between the coil and BNC, as well as the complex electromagnetic environment in the laboratory. It can be concluded that increasing the coil radius can lengthen the effective transfer distance, but the increase in coil radius is constrained in a limited range.

To verify the design and optimization flowcharts, the optimized CMR-WPT system is compared with the previous result [19], as shown in Fig. 20 and Table 5.

In Fig. 20, the experimental results are well consistent with the simulation analyses. In Table 5, the PTE of the designed CMR-WPT system at 6.78 MHz is 1.21% higher. In fact, an additional inner coil was incorporated with Tx coil in [19]. In this paper, the Tx and Rx coils were designed according to the flowcharts proposed in Section III.dD. As a result, a higher PTE was achieved, and the complexity and cost of the system were significantly reduced.

V. CONCLUSION

- With the same coil parameters and similar inductances, the plane square and plane spiral coils have satisfying performances in terms of effective transfer distance and PTE, but the magnetic field distribution of plane square is uneven.
- At 6.78 MHz and under the load of 50 Ω, as the coil radius and the number of turns increase, the effective transfer distance may increase to its maximum but then decrease, and the pitch is proportional to PTE. As the pitch increases, the PTE will be improved.
- In the processes of design and optimization, the effective transfer distance is determined by coil impedance. Moreover, the proposed flowcharts can be well applied in the actual WPT engineering to realize a longer effective transfer distance and a higher PTE.

REFERENCES

[1] A. Kurs, A. Karalis, R. Moffatt, J. D. Joannopoulos, P. Fisher, and M. Soljacic, "Wireless power transfer via strongly coupled magnetic resonances," *Science*, vol. 317, no. 5834, pp. 83–86, Jul. 2007.

[2] T. D. Ponnimbaduge Perera, D. N. K. Jayakody, S. K. Sharma, S. Chatzinotas, and J. Li, "Simultaneous wireless information and power transfer (SWIPT): Recent advances and future challenges," *IEEE Commun. Surveys Tuts.*, vol. 20, no. 1, pp. 264–302, 1st Quart., 2018.

[3] A. A. Eteng, S. K. A. Rahim, C. Y. Leow, S. Jayaprakasam, and B. W. Chew, "Low-power near-field magnetic wireless energy transfer links: A review of architectures and design approaches," *Renew. Sustain. Energy Rev.*, vol. 77, pp. 486–505, Sep. 2017.

[4] T. Campi, S. Cruciani, F. Maradei, and M. Feliziani, "Near-field reduction in a wireless power transfer system using LCC compensation," *IEEE Trans. Electromagn. Compat.*, vol. 59, no. 2, pp. 686–694, Apr. 2017.

[5] S. Y. R. Hui, W. Zhong, and C. K. Lee, "A critical review of recent progress in mid-range wireless power transfer," *IEEE Trans. Power Electron.*, vol. 29, no. 9, pp. 4500–4511, Sep. 2014.

[6] Z. Bi, T. Kan, C. C. Mi, Y. Zhang, Z. Zhao, and G. A. Keoleian, "A review of wireless power transfer for electric vehicles: Prospects to enhance sustainable mobility," *Appl. Energy*, vol. 179, pp. 413–425, Oct. 2016.

[7] G. Monti, M. V. De Paolis, L. Corchia, and L. Tarricone, "Wireless resonant energy link for pulse generators implanted in the chest," *IET Microw., Antennas Propag.*, vol. 11, no. 15, pp. 2201–2210, Dec. 2017.

[8] S. H. Kang, V. T. Nguyen, and C. W. Jung, "Analysis of MR-WPT using planar textile resonators for wearable applications," *IET Microw., Antennas Propag.*, vol. 10, no. 14, pp. 1541–1546, Nov. 2016.

[9] Y. Ben Fadhel, S. Ktata, K. Sedraoui, S. Rahmani, and K. Al-Haddad, "A modified wireless power transfer system for medical implants," *Energies*, vol. 12, no. 10, p. 1890, 2019.

[10] D. H. Tran, V. B. Vu, and W. Choi, "Design of a high-efficiency wireless power transfer system with intermediate coils for the on-board chargers of electric vehicles," *IEEE Trans. Power Electron.*, vol. 33, no. 1, pp. 175–187, Jan. 2018.

[11] Y. Li, W. Dong, Q. Yang, J. Zhao, L. Liu, and S. Feng, "An automatic impedance matching method based on the feedforward-backpropagation neural network for a WPT system," *IEEE Trans. Ind. Electron.*, vol. 66, no. 5, pp. 3963–3972, May 2019.

[12] Y. Li, S. Jiang, X.-L. Liu, Q. Li, W.-H. Dong, J.-M. Liu, and X. Ni, "Influences of coil radius on effective transfer distance in WPT system," *IEEE Access*, vol. 7, pp. 125960–125968, 2019.
[13] S. Assawaworrarit, X. Yu, and S. Fan, "Robust wireless power transfer using a nonlinear parity–time-symmetric circuit," *Nature*, vol. 546, no. 7658, pp. 387–390, Jun. 2017.
[14] J. Kim and J. Jeong, "Range-adaptive wireless power transfer using multiloop and tunable matching techniques," *IEEE Trans. Ind. Electron.*, vol. 62, no. 10, pp. 6233–6241, Oct. 2015.
[15] G. Lee, B. H. Waters, Y. G. Shin, J. R. Smith, and W. S. Park, "A reconfigurable resonant coil for range adaptation wireless power transfer," *IEEE Trans. Microw. Theory Techn.*, vol. 64, no. 2, pp. 624–632, Sep. 2016.
[16] K. Sasaki, S. Sugiura, and H. Iizuka, "Distance adaptation method for magnetic resonance coupling between variable capacitor-loaded parallel-wire coils," *IEEE Trans. Microw. Theory Techn.*, vol. 62, no. 4, pp. 892–900, Apr. 2014.
[17] K. Lee and S. H. Chae, "Power transfer efficiency analysis of intermediate-resonator for wireless power transfer," *IEEE Trans. Power Electron.*, vol. 33, no. 3, pp. 2484–2493, Mar. 2018.
[18] X. Chen, L. Chen, W. Ye, and W. Zhang, "Three-coil magnetically coupled resonant wireless power transfer system with adjustable-position intermediate coil for stable transmission characteristics," *J. Power Electron.*, vol. 19, no. 1, pp. 211–219, 2019.
[19] W. Zhong, C. K. Lee, and S. Y. R. Hui, "General analysis on the use of Tesla's resonators in domino forms for wireless power transfer," *IEEE Trans. Ind. Electron.*, vol. 60, no. 1, pp. 261–270, Jan. 2013.
[20] T.-H. Kim, G.-H. Yun, W. Y. Lee, and J.-G. Yook, "Asymmetric coil structures for highly efficient wireless power transfer systems," *IEEE Trans. Microw. Theory Techn.*, vol. 66, no. 7, pp. 3443–3451, Jul. 2018.
[21] D. Ahn and S. Hong, "A transmitter or a receiver consisting of two strongly coupled resonators for enhanced resonant coupling in wireless power transfer," *IEEE Trans. Ind. Electron.*, vol. 61, no. 3, pp. 1193–1203, Mar. 2014.
[22] D.-H. Kim, J. Kim, and Y.-J. Park, "Optimization and design of small circular coils in a magnetically coupled wireless power transfer system in the megahertz frequency," *IEEE Trans. Microw. Theory Techn.*, vol. 64, no. 8, pp. 2652–2663, Sep. 2016.
[23] S. Wang, Z. Hu, C. Rong, C. Lu, X. Tao, J. Chen, and M. Liu, "Optimisation analysis of coil configuration and circuit model for asymmetric wireless power transfer system," *IET Microw., Antennas Propag.*, vol. 12, no. 7, pp. 1132–1139, Jun. 2018.
[24] M. Lu and K. D. T. Ngo, "Systematic design of coils in series–series inductive power transfer for power transferability and efficiency," *IEEE Trans. Power Electron.*, vol. 33, no. 4, pp. 3333–3345, Apr. 2018.
[25] C. M. Zierhofer and E. S. Hochmair, "Geometric approach for coupling enhancement of magnetically coupled coils," *IEEE Trans. Biomed. Eng.*, vol. 43, no. 7, pp. 708–714, Jul. 1996.
[26] M. Zargham and P. G. Gulak, "Maximum achievable efficiency in near-field coupled power-transfer systems," *IEEE Trans. Biomed. Circuits Syst.*, vol. 6, no. 3, pp. 228–245, Jun. 2012.

YANG LI received the B.E., M.E., and Ph.D. degrees in electrical engineering from the Hebei University of Technology, Tianjin, China, in 2002, 2005, and 2013, respectively.

He is currently a Professor with the School of Electrical Engineering and Automation, Tiangong University, Tianjin. His current research interest includes wireless power transfer and its application.

SHAN JIANG was born in Hebei, China, in 1994. He received the B.S. degree in electrical engineering and automation from the School of Electrical Engineering and Automation, Hebei University of Technology, Tianjin, China, in 2016. He is currently pursuing the M.E. degree in electrical engineering with the School of Electrical Engineering and Automation, Tiangong University, Tianjin.

His current research interests include wireless power transfer and its applications.

JIA-MING LIU was born in Heilongjiang, China, in 1995. He received the B.S. degree in electrical engineering and automation from Tiangong University, Tianjin, China, in 2017, where he is currently pursuing the M.E. degree in electrical engineering. His current research interest includes wireless power transfer and its applications.

XIN NI was born in Tianjin, China, in 1995. He received the B.S. degree in automation from Tiangong University, Tianjin, in 2017, where he is currently pursuing the M.E. degree in electrical engineering.

His current research interest includes wireless power transfer and its applications.

RUI WANG was born in Heilongjiang, China, in 1996. He received the B.S. degree in automation from Tiangong University, Tianjin, China, in 2018, where he is currently pursuing the M.E. degree in electrical engineering.

His current research interest includes wireless power transfer and its applications.

JING-NAN MA was born in Hebei, China, in 1996. He received the B.S. degree in electrical engineering and automation from the School of Electrical Engineering and Automation, Hebei University of Science and Technology, Hebei, in 2018. He is currently pursuing the M.E. degree in electrical engineering with the School of Electrical Engineering and Automation, Tiangong University, Tianjin, China.

His current research interest includes wireless power transfer and its applications.